The Accumulated Response of Deciduous *Liquidambar formosana* Hance and Evergreen *Cyclobalanopsis glauca* Thunb. Seedlings to Simulated Nitrogen Additions

Zhenzhen Zhang[1]*, Yamin Zhao[1], Xiaoyan Zhang[1], Sichen Tao[1], Xiong Fang[2], Xingwen Lin[1], Yonggang Chi[1], Lei Zhou[1] and Chaofan Wu[1]

[1] College of Geography and Environmental Sciences, Zhejiang Normal University, Jinhua, China, [2] Fujian Provincial Key Laboratory of Soil Environmental Health and Regulation, College of Resources and Environment, Fujian Agriculture and Forestry University, Fuzhou, China

Nitrogen depositions in the Yangtze River Delta have is thought to shift the coexistence of mixed evergreen and deciduous species. In this study, the seedlings of the dominant evergreen species *Cyclobalanopsis glauca* Thunb. and the deciduous species *Liquidambar formosana* Hance from the Yangtze River Delta were chosen to test their responses to simulated N additions using an ecophysiological approach. N was added to the tree canopy at rates of 0 (CK), 25 kg N ha^{-1} year^{-1} (N25), and 50 kg N ha^{-1} year^{-1} (N50). The leaf N content per mass (N_m, by 44.03 and 49.46%) and total leaf chlorophyll content (*Chl*, by 72.15 and 63.63%) were enhanced for both species, and *C. glauca* but not *L. formosana* tended to allocate more N to *Chl* per leaf area (with a higher slope). The enhanced N availability and *Chl* promoted the apparent quantum yield (*AQY*) significantly by 15.38 and 43.90% for *L. formosana* and *C. glauca,* respectively. Hydraulically, the increase in sapwood density (ρ) for *L. formosana* was almost double that of *C. glauca*. Synchronous improved sapwood specific hydraulic conductivity (K_S, by 37.5%) for *C. glauca* induced a significant reduction in stomatal conductance (g_s) ($p < 0.05$) in the N50 treatments, which is in contrast to the weak varied g_s accompanied by a 59.49% increase in K_S for *L. formosana*. As a result, the elevated maximum photosynthesis (A_{max}) of 12.19% for *L. formosana* in combination with the increase in the total leaf area (indicated by a 37.82% increase in the leaf area ratio-leaf area divided by total aboveground biomass) ultimately yielded a 34.34% enhancement of total biomass. In contrast, the A_{max} and total biomass were weakly promoted for *C. glauca*. The reason for these distinct responses may be attributed to the lower water potential at 50% of conductivity lost (P_{50}) for *C. glauca*, which enables higher hydraulic safety at the cost of a weak increase in A$_{max}$ due to the stomatal limitation in response to elevated N availability. Altogether, our results indicate that the deciduous *L. formosana* would be more susceptible to elevated N availability even if both species received similar N allocation.

Keywords: evergreen and deciduous species, nitrogen addition, biomass, hydraulic changes, gas exchange

INTRODUCTION

Evergreen and deciduous broad-leaved tree species can coexist across a variety of landscapes around the globe and play important roles in forest structure and functions (Wang et al., 2007; Kikuzawa et al., 2013; Ouédraogo et al., 2016). In these coexistent ecosystems, they usually differ in ecological habits, which contributes to the explanation of the mechanisms by which these two groups coexist (Xie et al., 2012; Devi and Garkoti, 2013; Álvarez-Yépiz et al., 2017). In recent decades, the fertilization effect of nitrogen deposition in forest ecosystems has received increasing attention (Wang and Feng, 2005; Zhang, 2006) and has been recognized as a threat to plant diversity in these mixed forests (Bobbink et al., 2010; Hietz et al., 2011; Liu et al., 2013a; Lu et al., 2014). As reported, the global nitrogen deposition in the end of last century was already exceeded 25 kg^{-1} ha^{-1} yr^{-1} (Binkley et al., 2004), and will be doubled in the end of this decade (Deutsch and Weber, 2012). However, the underlying mechanisms have rarely been discussed in previous studies (Takashima et al., 2004; Palmroth et al., 2014). Evergreen and deciduous species usually specialize their habitats and survival strategies for the tradeoff between photosynthetic capacity and persistence (Takashima et al., 2004; Shipley et al., 2006; Curtis and Ackerly, 2008). This specialization could enable the deciduous species with higher demands for nitrogen acquisition to photosynthesize more efficiently and allow evergreen trees to invest more N in the durable leaves that can persist through disturbances (Pringle et al., 2011). The existing evidence across 231 evergreen species and 110 deciduous species has already shown higher N enrichment for the latter due to the added N (Xia and Wan, 2008). Thus, we could expect that the deciduous species would also accumulate more leaf N than the evergreen species in the coexistent ecosystems. In addition, the evergreen and deciduous species also differ in the fraction of N investment in photosynthesis. Evidence has indicated that the photosynthetic N use efficiency (PNUE) is much lower for evergreen species than for deciduous species, which was primarily ascribed to the smaller fraction of nitrogen allocated to the photosynthetic apparatus, such as chlorophyll content, in evergreen species (Takashima et al., 2004; Hu et al., 2008). Comparably higher nitrogen content and specific leaf area (SLA) for the deciduous species enable their stronger morphology and photosynthetic plasticity (Hu et al., 2008). Therefore, this evidence supports the increased opportunity for deciduous species to take advantage of high N conditions (Takashima et al., 2004).

However, uncertainties still exist because disturbances such as seasonal drought could negate the fertilization effect for deciduous species by removing the ability to utilize elevated N (Wang et al., 2012a; Liu et al., 2013b). The underlying physiological reasons may be attributed to the different hydraulic tolerances in response to drought (Pivovaroff et al., 2016). The deciduous species possessed hydraulic architecture typical of drought-sensitive plants, i.e., low wood density, wider xylem vessels, higher sapwood-specific hydraulic conductivity (K_S), and high vulnerability to drought-induced embolism (Choat et al., 2004; Kröber et al., 2015). In contrast, the evergreen species had lower K_S and leaf specific conductivity but were less susceptible to embolism (Choat et al., 2004; Chen et al., 2008). These differences would lead to stronger stomatal limitations for the deciduous species in dry conditions (Brodribb et al., 2002; Zhang et al., 2013; Kröber and Bruelheide, 2014). In addition, due to the fertilization effect, elevated photosynthesis leads to fast growth as well as decreased wood density and increased stem hydraulic conductivity (Pivovaroff et al., 2016), which potentially enhances the vulnerability of deciduous species in response to seasonal drought (Bauer et al., 2001; Wang et al., 2012b).

As a developing country during past decades, China has also experienced the most severe atmospheric nitrogen deposition in the world due to the rise of anthropogenic nitrogen release (Liu et al., 2013b; Lu et al., 2018). In particular, the Yangtze River Delta region, where urbanization is highly developed, is crucial for nitrogen deposition (Liu et al., 2013b), since the nitrogen deposition rates reached an level of 38.4 $^{kg\ ha-1\ yr-1}$ in the end of last century (Zhou et al., 2001). In this study, we focused on the morphological and physiological responses of deciduous and evergreen species to the abundance of nitrogen to investigate whether the former could take advantage of the fertilization effect more fully due to seasonal drought disturbance. We hypothesized that:
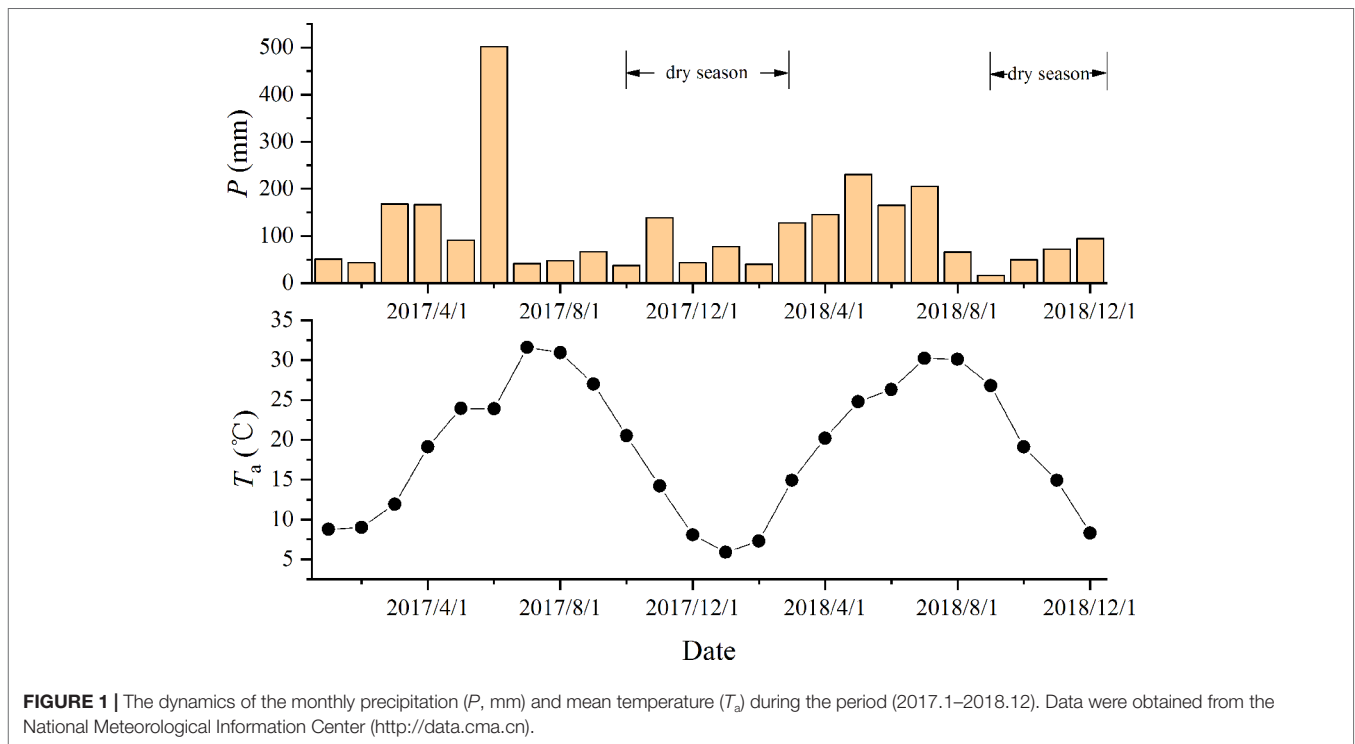
1. The resource acquisition and utilization strategies of deciduous species will make them more susceptible to the added N, thus leading to a higher increase in leaf N and chlorophyll content than observed in the evergreen species.
2. Meanwhile, the increased stem conductivity and decreased wood density of deciduous species will lead to stronger stomatal limitation, which will neutralize the increase in leaf photosynthesis as well as the overall biomass.

Understanding the effects of N deposition on plant physiological processes for deciduous and evergreen species may illuminate the mechanisms behind overall forest responses to global changes.

MATERIALS AND METHODS

Site Descriptions

The study was conducted in the Dashu Garden in Jinhua, Zhejiang Province (119.79°E, 29.16°N), which is characterized by a subtropical monsoon climate with an average annual temperature of 17.3°C and an average annual precipitation of 1,300–1,600 mm. The elevation was 163 m and the soil was typical yellow soil. Located at the margin of temperate and subtropical zones, the vegetation is mostly covered by evergreen and deciduous broad-leaved mixed forests. The dry season starts in September and continues into March of the next year (**Figure 1**). In January 2017, seedlings of two dominant species, *Cyclobalanopsis glauca* Thunb. (evergreen broad-leaved) and *Liquidambar formosana* Hance (deciduous broad-leaved) were planted in holes (50 cm in diameter and 50 cm in depth) to carry out the simulated nitrogen addition experiments. In order to manipulate the original growth habitats of the two species more closely and ensure the water uptake from the deep soil, the typical mountainous red-yellow soil was moved from the secondary bare land in North Mountain,

FIGURE 1 | The dynamics of the monthly precipitation (P, mm) and mean temperature (T_a) during the period (2017.1–2018.12). Data were obtained from the National Meteorological Information Center (http://data.cma.cn).

which was 1 km away from our site, and fully mixed into planting substrate in the hole.

Current N deposition rate in tropical forests of southern China is reported to range from 15 to 73 g N m^{-2} a^{-1} (Zhang et al., 2008), while the total deposition in our site was 2.69 g N m^{-2} a^{-1} (Xu et al., 2015). To simulate natural nitrogen deposition that might occur in the future, three treatments were designed, including the control group (CK), 25 gN m^{-2} a^{-1} (N25), and 50 gN m^{-2} a^{-1} (N50) (nitrogen from atmospheric deposition was not included); each had five replicates. Each replicate consisted of 10 individuals of 2-year-old seedlings. The experiment was started in April 2017. The NH$_4$NO$_3$ solutions were evenly sprayed from the canopy at the middle and the end of each month until October 2018. During the period of defoliation for *L. formosana* (November 2017 to March 2018), the NH$_4$NO$_3$ solution was sprayed onto the surface of the soil. In order to exclude the influence of changed water -regime, no extra water was input to the plots except for the rain. Weeding was carried out during the experiment to minimize the interference caused by other factors. After the N treatment was stopped, the leaves of both species were in good condition, indicating that the leaves were not significantly damaged.

Gas Exchange and Leaf Water Potential

The gas exchange measurements were carried out from 9:30 to 11:30 on typical sunny days from October 11 to October 20, 2018. The photosynthetic light response curve was measured in the fully developed mature leaves ($n=15$ for each treatment) using a portable photosynthesis system (LiCOR 6800, LiCOR Biosciences, Lincoln, NE, USA). The light intensity intervals were set as 0, 100, 200, 400,

600, 800, 1,000, 1,200, 1,500 μmol·m^{-2}·s^{-1}, and the temperature was 25°C. The flow rate was set at 500 μmol s^{-1}, and the CO$_2$ concentration was set at 500 μmol·mol^{-1}. We use a nonorthogonal hyperbolic model to obtain the light response curve parameters:

$$A = \frac{1}{2\theta}\left(AQYI + A_{max,g} - \sqrt{(AQYI +_{max,g})^2 - 4\theta AQYIA_{max,g}}\right) - R_d$$
(1)

A is the CO$_2$ gas exchange rate (μmol CO$_2$ m^{-2}s^{-1}), I is the instantaneous light intensity (μmol m^{-2} s^{-1}), apparent quantum yield (AQY) is the apparent quantum yield, $A_{max,g}$ is the assimilation rate under saturating light (μmol CO$_2$ m^{-2}s^{-1}), θ is the curvature, and R_d is the dark respiration rate (the CO$_2$ exchange rate at I=0, μmol CO$_2$ m^{-2}s^{-1}). We also recorded stomatal conductance (g_s, mol m^{-2} s^{-1}) and intercellular CO$_2$ concentrations (C_i, μmol m^{-2} s^{-1}).

Daily courses of leaf instantaneous net photosynthetic rate (A_i, μmol CO$_2$ m^{-2}s^{-1})), g_s, and transpiration rate (E_t, μmol m^{-2} s^{-1}) were measured at 2 h intervals from 5:00 am to 17:00 pm during October 22 to October 25 on 5 seedlings of each N treatment. Meanwhile, leaf water potential (Ψ_L, Mpa) of the detached shoots was synchronously measured with a pressure chamber (PMS, Albany, OR, USA) after the instantaneous gas exchange measurements.

Hydraulic Conductivity and Sap Wood Density

The current year branches were cut off (30 cm length) from each sampled tree ($n=15$). All branches were covered with black

plastic bags to prevent water loss before they were immediately transported to the laboratory to determine the sapwood hydraulic conductivity (K_S, g cm MPa^{-1} min^{-1} cm^{-2}) with a high pressure flow meter (HPFM Gen3; Dynamx Corp., Elkhart, Indiana, USA). The specific experimental operations are as follows:

First, all the samples were cut off underwater at approximately 5 cm from the base. Then, the tree bark was removed approximately 3 cm from the sample ends. Emboli were removed from samples by vacuum infiltration under solution consisting of 0.22 µm filtered and degassed, distilled water for 8 h before being connected to HPFM under purified water (Barnard et al., 2011). Under the quasi-steady-state mode, deionized water purified by the Water Purification System (Milli-Q Advantage, Merk Millipore, Germany) was degassed and injected into the branches through HPFM at a pressure of 0.5 MPa until a stable flow rate appeared (approximately 5 to 10 min) to obtain the maximum whole-shoot level hydraulic conductance (K_h, g cm MPa^{-1} min^{-1}). After the measurements, the base diameter (d, mm) was measured with a vernier caliper to obtain the cross-sectional area (A_S, cm^2) of the base of the shoot, and the maximum sapwood hydraulic conductivity K_S (g cm MPa^{-1} min^{-1} cm^2) was calculated as:

$$K_S = K_h / A_s \qquad (2)$$

Five segments of 3 cm length for each branch were collected to measure the sap wood density (ρ, g cm^{-3}). The fresh volume (V, cm^3) of these wood segments was determined gravimetrically by water displacement according to Archimedes' principle after removing the bark and phloem (Osazuwa-Peters and Zanne, 2011). All samples were then oven-dried at 105°C for 24 h to get the dry weight (G, g). The sapwood density was calculated as $\rho = G/V$.

Stem xylem vulnerability was measured using the centrifuge method (Cochard et al., 2005; Sperry et al., 2012). After determining the maximum K_S, a centrifugal machine (Sorvall RC-5C; Thermo Fisher Scientific, Waltham, MA, USA) equipped with a custom rotor (Alder et al., 1997) that was able to spin the stem segments was used to induce negative xylem pressure and induce cavitation. Hydraulic conductivity was measured between each induced pressure, and the percent loss of conductivity under a certain negative pressure (PLC_i, %) was calculated as:

$$PLC_i = 100 \times K_{hi} / K_{max} \qquad (3)$$

where K_{hi} (g cm MPa^{-1} min^{-1}) and K_{max} (g cm MPa^{-1} min^{-1}) refer to the K_h at certain negative pressures and maximum K_h. Vulnerability curves were constructed by plotting pressure *versus* PLC_i and fitting a Weibull model (Pammenter and Van der Willigen, 1998):

$$PLC = 100 / (1 + \exp(a(\Psi - b))) \qquad (4)$$

According to this equation, water potential at 50% of conductivity lost (P_{50}, MPa^{-1}) was determined for each species.

The Leaf Economic Traits

One hundred foliage round pieces were collected for 10–20 mature leaves with a hole puncher (10 mm in diameter) for each species in each treatment and were placed in the oven in an envelope for 24 h. The foliage rounds were weighed to estimate the (cm^2 g^{-1}). The remaining leaves in another envelope B. Five to 10 leaves were taken from the remaining leaves of each shoot and cut into slices with a width of 0.5 mm (0.2–0.5 g). The leaf chlorophyll of these samples was extracted with a mixed solution (acetone:ethanol = 2:1) for approximately 24 h until they turned white. Then, a spectrophotometer was used to measure the absorbance of the supernatant liquid. The calculation of the total chlorophyll content (*Chl* (mg m^{-2}), chlorophyll a + chlorophyll b) followed the description in Zhang et al. (2017). All the leaves, including those measured for leaf chlorophyll and *SLA,* on each shoot were then collected and dried in the oven at 65°C for 24 h and weighed for leaf dry mass (M_L, g). The multiples of M_L and the *SLA* for each shoot were used obtain the total leaf area (A_L, m^2), which was used to calculate the ratio of leaf area to sapwood area (A_L/A_S, m^2 cm^{-2}).

The dried leaves were ground into powder and analyzed for N content as a mixed sample by an elemental analyzer (EA Flash 1112; Thermo Fisher Scientific). The nitrogen content per unit area (N_a, g m^{-2}) and the nitrogen content per unit mass were calculated (N_m, mg g^{-1}).

The Whole Tree Biomass

To estimate the whole tree biomass, 15 sample trees were selected from each group and harvested to obtained the above-ground and underground total biomass (except fine roots) by calculating the total biomass of the leaves and the root-shoot ratio of each sample tree. Then, we calculated the leaf mass fraction (*LMF*, %) and the leaf area ratio (*LAR*, m^2 g^{-1}), of which total the leaf area is the product of *SLA* and the total biomass.

Data Analysis and Processing

Analysis of variance (ANOVA) was conducted on all the traits measured above with SPSS 25 (version 25.0, IBM SPSS Inc., Chicago, USA) to examine the treatment effects ($n = 3$) for different species. The relationship between the *SLA*, *Chl*, A_{max}, and g_s values and N_a and N_m across the two species and three treatments were also fitted to analyze the convergence of leaf functional traits due to the elevated N availability. We also regressed A_{max} and K_S with g_s for the different species in each treatment to verify the variation of the coordination relationship between shoots and leaves in response to N addition. In these analyses, individual sample points (or leaves) were used. Where a significant relation between any two variables was found ($p < 0.05$), we re-analyzed the data with analysis of covariance (ANCOVA) allowing the slope and intercept to vary among treatments. Therefore, in our analysis, a single curve indicates that the treatments or tree species have the same fitted relationship (i.e., the interaction items in the ANCOVA analysis are not statistically significant, $p > 0.05$).

RESULTS

Effects of N Additions on Leaf Economics

As shown in **Figure 2**, the *SLA* variation was well explained by the N_m of each species along the treatments (p < 0.05 for all the relations based on the ANCOVA analysis). Of note, the data in N25 and N50 shared the same relations for *L. formosana*. The mean *SLA* for *L. formosana* in the highest N treatments (N50) was 184.66 cm^2 g^{-1}, which was 35.99% higher than the unfertilized treatment CK (*p* < 0.01, **Table 1**). Similarly, the mean *SLA* for *C. glauca* increased 34.72% in the N50 treatments compared with the CK treatments (p < 0.01, **Table 1**). In addition, the ratio of leaf area to sapwood area (A_L/A_S) was also enhanced by 26.06% for *L. formosana* but not for *C. glauca* (**Table 1**).

The fertilization significantly increased the mean leaf N_m (*p* < 0.01, **Table 1**) and N_a (*p* < 0.05, **Table 1**, except for *L. formosana*), which further enhanced the *Chl* in the N50 treatments by 72.15 and 63.63% for *L. formosana* and *C. glauca* respectively. The mean N_m of *L. formosana* leaves increased 44.03% from 16.92 mg g^{-1} in the CK treatment to 24.37 mg g^{-1} in the highest fertilized N50 treatments. The corresponding increase in *C. glauca* was 49.46% (from 9.24 to 13.81 mg g^{-1}). The difference in N_a between CK and N50 of *L. formosana* was not significant (*p* > 0.05), but it was 32.10% for *C. glauca*.

Differences in N_a across treatments and species were clearly presented by the relations between *Chl* and leaf N (**Figure 3**). For each treatment, the concentration of *Chl* closely responded to the variations of N_a for the *L. formosana* with different slopes (p < 0.05, ANCOVA), which ranged from the lowest of 31.68 in the CK treatment to the highest of 116.83 in the N50 treatment. The relationship was consistent among treatments for *C. glauca* (*p* < 0.01, ANCOVA). On an area basis, the ratio of *Chl* to N_a increased 40 and 22.2% for *L. formosana* and *C. glauca* from CK to N50, indicating the higher allocation of newly acquired N to photosynthetic functions for the deciduous *L. formosana*.

Variation in Photosynthetic Capacity and Water Transport Capacity

According to the light response curve, C_i decreased by 11.64 and 42.04% for *L. formosana* and *C. glauca,* respectively. Meanwhile, *AQY* increased by 15.38 and 43.90%, respectively. The g_s decreased by 37.5% in the N50 treatments for *C. glauca* but was not significant for *L. formosana* (only 8.33%, *p* > 0.05) (**Table 1**). Among the treatments, the A_{max} for *L. formosana* increased 12.19% from CK to N50, whereas this enhancement was not observed in *C. glauca*. Qualitatively, the treatment means of A_{max} were found to increase with *SLA* and N_m for *L. formosana* but were not significant for *C. glauca*, while the g_s was reduced by the enhancement of *SLA* and N_m only for *C. glauca* (*p* < 0.05, **Figure 4**). In addition, the relationship between A_{max} and g_s was altered in the N50 (**Figure 5A**), where the A_{max} for *L. formosana* tended to be more sensitive to the increase in g_s when g_s < 0.15 mol m^{-2} s^{-1}, and A_{max} for *C. glauca* tended to rapidly decrease when g_s > 0.06 mol m^{-2} s^{-1} (**Figure 5A**).

In agreement with the enhanced A_{max} (albeit not significantly so for *C. glauca*), the water transport capacity per sapwood area (K_S) increased by 59.49 and 39.18% for *L. formosana* and *C. glauca,* respectively. Surprisingly, the improved water transport capacity in the N50 treatments tended to maintain higher and lower g_s sensitivity for *L. formosana* and *C. glauca,* respectively (**Figure 5B**).

Daily Dynamics of Gas Exchange and Water Relations

The light was increased on a daily basis before 9:00, and g_s and E_t were enhanced in the highest N treatments for both species (**Figure 6**). Notably, even g_s for both species also experienced a rapid reduction at 11:00, which may be attributed to the lowest Ψ_L at this time, while the recovery of the g_s after the replenishment of the Ψ_L at 13:00 only occurred for *L. formosana*, which also maintained higher E_T at the same time (**Figure 6**). In contrast, the g_s and E_t for *C. glauca* persistently decreased until
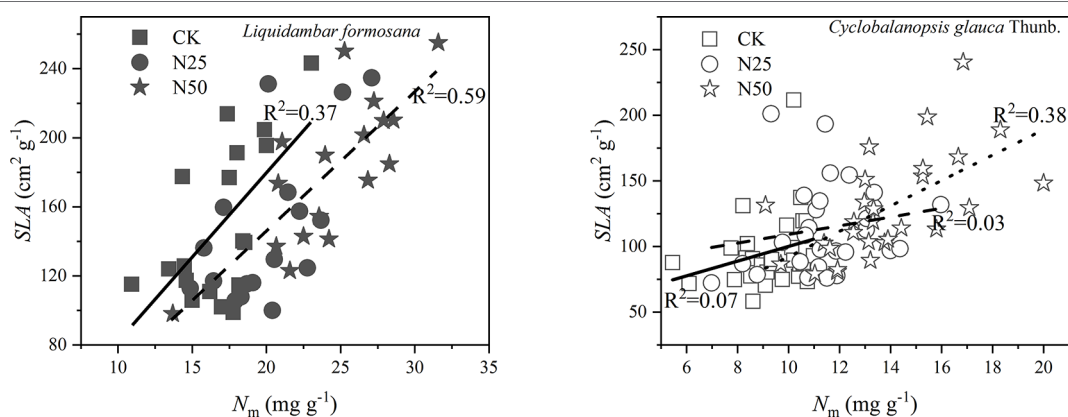
FIGURE 2 | The specific leaf area (*SLA*) as samples of ten leaves averaged for each individual of *Cyclobalanopsis glauca* Thunb. and *Liquidambar formosana* selected for gas exchange measurements as a function of leaf N per unit mass (N_m). Solid lines fit linearly to the CK data, broken lines fit linearly to the N25 data, and dotted line fit linearly to the N50 data. Of note, the data of N25 and N50 share the same relations for *L. formosana*.

TABLE 1 | Treatment means of light-saturated CO_2 exchange rate (A_{max}), stomatal conductance (g_s), intercellular CO_2 (C_i), apparent quantum yield (AQY), leaf N per unit leaf mass (N_m) and per unit leaf area (N_a), total amount of chlorophyll (Chl) on a mass and area basis, leaf area per mass (SLA), hydraulic conductance (K_S), wood density (ρ), and the ratio of leaf area to sapwood area (A_L/A_S).

Traits	N treatments	*L. formosana*	*C. glauca*
A_{max} (μmol CO_2 m^{-2}s^{-1})	CK	12.63 (2.53)b	7.56 (1.35)a
	N25	11.87 (1.82)b	7.24 (2.16)a
	N50	14.17 (4.03)a	7.91 (2.49)a
g_s (mol H_2O m^{-2} s^{-1})	CK	0.12 (0.03)a	0.08 (0.01)a
	N25	0.11 (0.03)a	0.08 (0.02)a
	N50	0.11 (0.01)a	0.05 (0.02)b
C_i (μmol CO_2 mol^{-1})	CK	312.55 (15.67)a	327.69 (12.44)a
	N25	307.94 (17.76)ab	211.57 (16.49)b
	N50	276.17 (10.23)b	189.92 (13.55)b
AQY (μmol CO_2 μmol^{-1} PPFD)	CK	0.033 (0.004)b	0.041 (0.013)c
	N25	0.036 (0.011)ab	0.051 (0.017)b
	N50	0.039 (0.014)a	0.059 (0.019)a
N_m (mg g^{-1})	CK	16.92 (2.82)c	9.24 (0.69)b
	N25	20.09 (3.36)b	11.47 (0.95)ab
	N50	24.37 (4.19)a	13.81 (1.25)a
N_a (g m^{-2})	CK	1.22 (0.11)a	0.81 (0.32)a
	N25	1.30 (0.25)a	0.95 (0.24)ab
	N50	1.31 (0.22)a	1.07 (0.24)a
Chl (mg m^{-2})	CK	2.55 (0.53)b	1.43 (0.36)b
	N25	3.22 (0.78)b	1.62 (0.48)b
	N50	4.39 (0.67)a	2.34 (0.56)a
SLA (cm^2 g^{-1})	CK	135.78 (20.00)b	95.86 (14.73)b
	N25	152.68 (23.34)b	114.14 (16.92)ab
	N50	184.66 (14.67)a	129.14 (19.69)a
K_S (g cm MPa^{-1} min^{-1} cm^{-2})	CK	4.74 (2.11)b	3.42 (1.41)b
	N25	5.60 (2.24)ab	3.64 (0.86)ab
	N50	7.56 (1.99)a	4.76 (0.67)a
ρ (g ml^{-1})	CK	0.53 (0.07)a	0.61 (0.06)a
	N25	0.47 (0.07)b	0.55 (0.06)ab
	N50	0.41 (0.09)b	0.53 (0.04)b
A_L/A_S (m^2 cm^{-2})	CK	4.72 (0.79)b	3.56 (0.83)a
	N25	5.18 (1.14)ab	4.24 (0.71)a
	N50	5.95 (0.98)a	3.72 (0.66)a

Different letters indicate differences at p < 0.05, N25, plots with N additions of 25 kg ha^{-1} year^{-1}; N50, plots with N additions of 50 kg ha^{-1} year^{-1}; CK, control treatments.

the end of the experiments. As a result, the E_t of *L. formosana* in the N50 treatments was apparently enhanced compared to that in the CK treatment, thus leading to excessive water loss (decreased lowest Ψ_L). The reduced E_t in the N50 from 11:00 to 17:00 for *L. formosana* maintained the water status compared to the CK treatments (stable lowest Ψ_L). These differences enable *L. formosana* to support higher photosynthesis in the N50 treatments, at the cost of exacerbated water stress. In contrast, the A_i that was elevated by the increased g_s before 9:00 for *C. glauca* tended to be neutralized after 11:00 in the N50, with the benefits of stable water status (**Figure 6**).
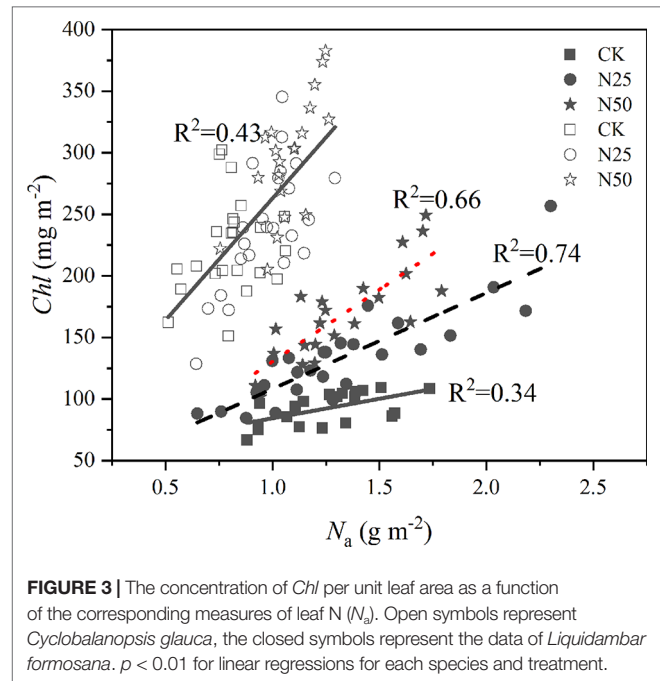
FIGURE 3 | The concentration of *Chl* per unit leaf area as a function of the corresponding measures of leaf N (N_a). Open symbols represent *Cyclobalanopsis glauca*, the closed symbols represent the data of *Liquidambar formosana*. $p < 0.01$ for linear regressions for each species and treatment.

Variation in Plant Biomass

In agreement with the enhanced leaf N_m, the total biomass of *L. formosana* individuals increased by 34.34% in the N50 treatment (**Figure 7**). In contrast, the growth of *C. glauca* was not affected by the enhanced N availability. In addition, the N concentration of plant biomass was found to increase by 86.57% (*L. formosana*) and 62.22% (*C. glauca*) in the N50 treatments. Similarly, the highest N addition rate increased the fraction of leaves to LAR (leaf area divided by total aboveground biomass) by 37.82% for *L. formosana* and 44.15% for *C. glauca*. Notably, the LMF (leaf mass/total aboveground biomass) did not change for either species, which was consistent with the increased leaf SLA across the two species (**Table 1**).
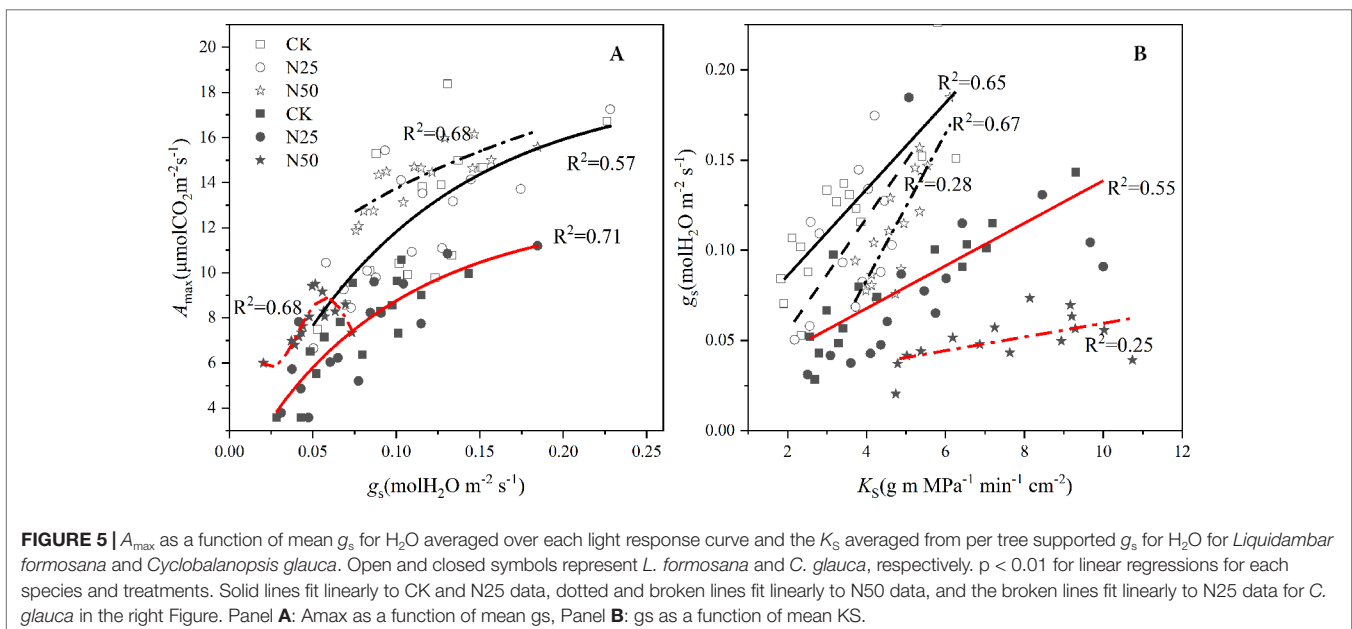
Hydraulic Changes

The ρ decreased by 21.56% (*L. formosana*) and 12.95% (*C. glauca*) between the CK treatments and the N50, indicating the reduced mechanical strength for both species due to the enhanced N availability. When the two species were compared, we found that the P_{50} was much lower for *C. glauca*, which indicated higher resistance to cavitation (**Figure 8**). *L. formosana* displayed an enhanced xylem vulnerability to cavitation (increased P_{50}) in the highest N treatments, which is in contrast to *C. glauca,* with weak variations.

DISCUSSION

The Accumulation and Allocation of Extra N

In N-saturated ecosystems, the extra N is considered to be weakly accumulated in plant tissues (Curtis and Ackerly, 2008). The subtropical region in China was thought to be N saturated

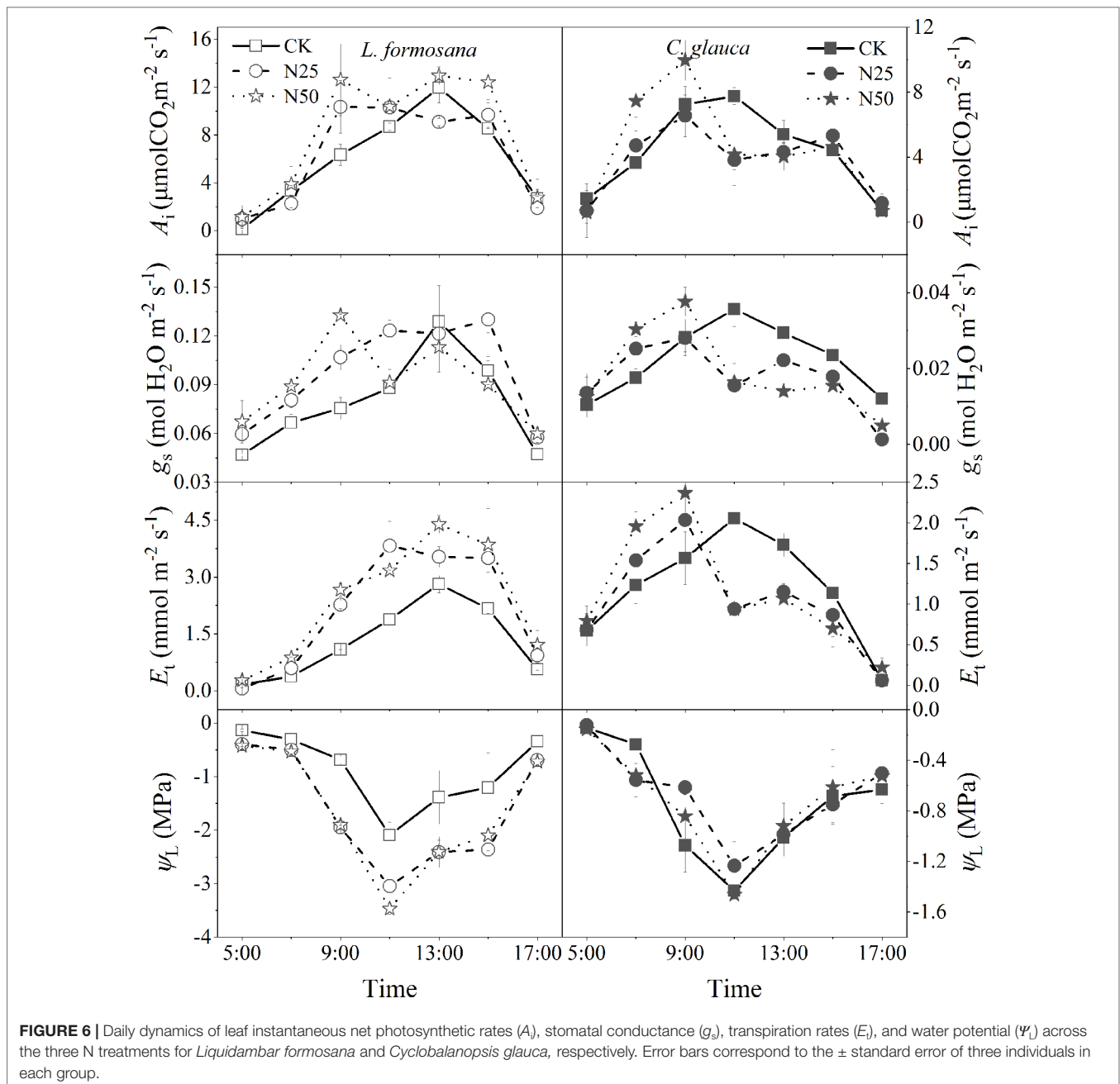**FIGURE 4 |** The averaged maximum CO_2 exchange rate per unit leaf under light-saturated conditions (A_{max}) and stomatal conductance for H_2O (g_s) across each light response curve as a function of specific leaf area (SLA) and leaf N per mass (N_m). Open and closed symbols represent the data of *Liquidambar formosana* and *Cyclobalanopsis glauca* leaves, respectively. The data are shown as the means ± SD.

FIGURE 5 | A_{max} as a function of mean g_s for H_2O averaged over each light response curve and the K_S averaged from per tree supported g_s for H_2O for *Liquidambar formosana* and *Cyclobalanopsis glauca*. Open and closed symbols represent *L. formosana* and *C. glauca*, respectively. $p < 0.01$ for linear regressions for each species and treatments. Solid lines fit linearly to CK and N25 data, dotted and broken lines fit linearly to N50 data, and the broken lines fit linearly to N25 data for *C. glauca* in the right Figure. Panel **A**: Amax as a function of mean gs, Panel **B**: gs as a function of mean KS.

during the past decades (Lu et al., 2014). However, unexpectedly, the mean leaf N_m and N_a were obviously enhanced in the N50 treatments for both *L. formosana* (44.03% for N_m) and *C. glauca* (49.46 and 32.10%) (**Table 1**). Meanwhile, the leaf chlorophyll

content was improved synchronously and was linearly related to the leaf N across the treatment and species (**Figure 3**), which revealed an enhanced ability to receive light energy, as presented in other studies (Xia and Wan, 2008; Tilman and Isbell, 2015;

FIGURE 6 | Daily dynamics of leaf instantaneous net photosynthetic rates (A_i), stomatal conductance (g_s), transpiration rates (E_t), and water potential (Ψ_L) across the three N treatments for *Liquidambar formosana* and *Cyclobalanopsis glauca,* respectively. Error bars correspond to the ± standard error of three individuals in each group.

Wooliver et al., 2016). These results may indicate that the N in the ecosystem was not saturated in this ecosystem, which is contradictory to previous studies conducted in tropical forests (Brookshire et al., 2012; Lu et al., 2018).

In addition, the weak changes in N_a for *L. formosana* compared to evergreen *C. glauca* contradict our hypothesis, even though the former still has higher leaf N ($p < 0.01$). The reason may be attributed to the increase in $A_L : A_S$ of 26.06% for *L. formosana*, but not for *C. glauca*, and N_m increased significantly (**Table 1**). The $A_L : A_S$ that reciprocal to the Huber value implied the supported leaf area by the sap wood per unit area. This implied the tendency of *L. formosana* to enhance its light acquisition ability to optimize

its carbon assimilation (Iversen and Norby, 2008). A study indicated a higher allocation to the photosynthetic apparatus in deciduous species (Takashima et al., 2004), which leads to a weak increase in N allocation per leaf area (**Table 1**).

On the basis of area, the allocation of N to *Chl* was found to vary across the two species (**Figure 3**). The N_a determined *Chl* was weakly related to the N treatments for *C. glauca*. Similar results have already been reported in another evergreen species, *Eucalyptus cladocalyx* (Myrtaceae) (Simon et al., 2010). A_{max} enhanced fraction of *Chl* in the N in the highest N treatments was found for *L. formosana* (**Figure 3**), which is consistent with our hypothesis (Xia and Wan, 2008). The preferential allocation by *L.*
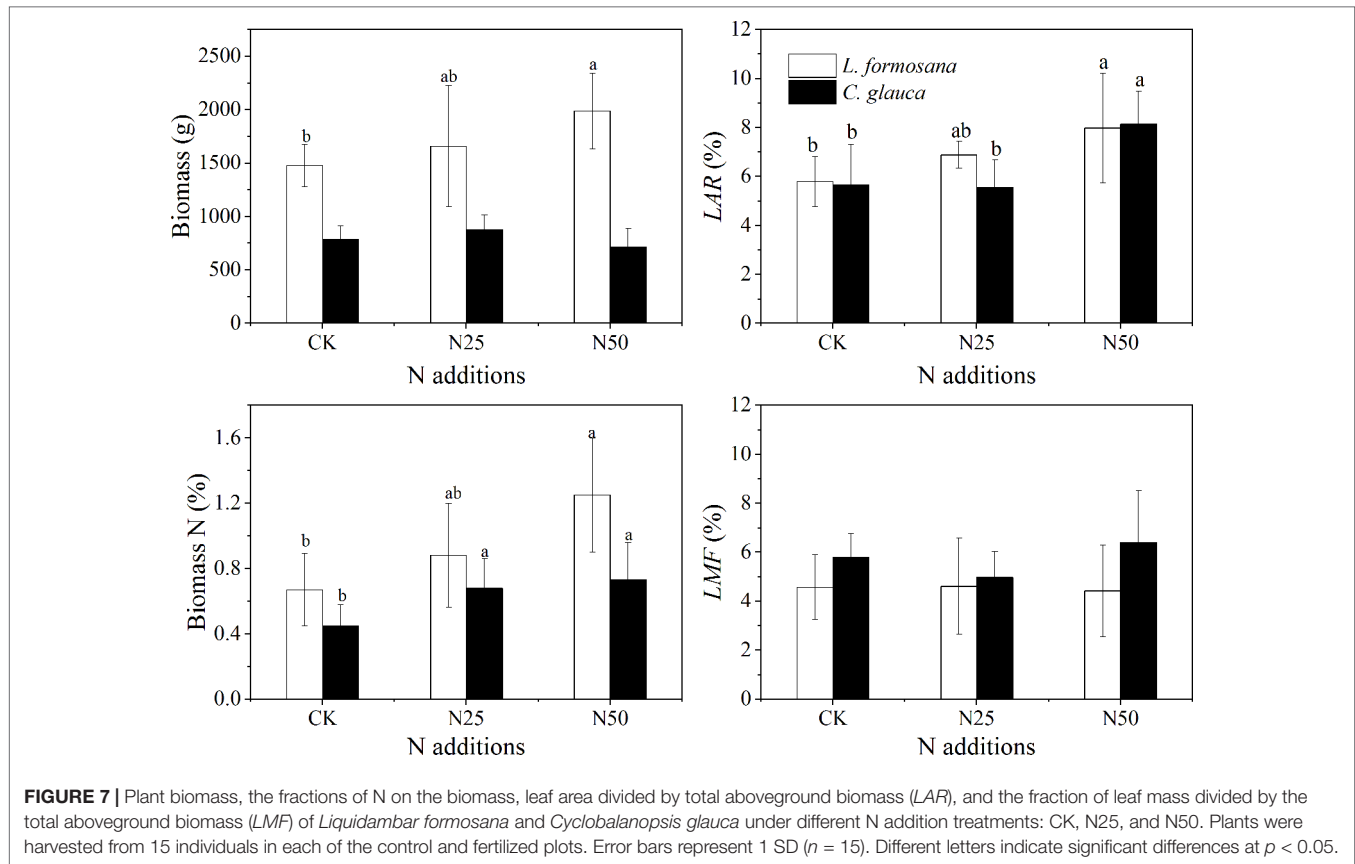
FIGURE 7 | Plant biomass, the fractions of N on the biomass, leaf area divided by total aboveground biomass (*LAR*), and the fraction of leaf mass divided by the total aboveground biomass (*LMF*) of *Liquidambar formosana* and *Cyclobalanopsis glauca* under different N addition treatments: CK, N25, and N50. Plants were harvested from 15 individuals in each of the control and fertilized plots. Error bars represent 1 SD (n = 15). Different letters indicate significant differences at $p < 0.05$.
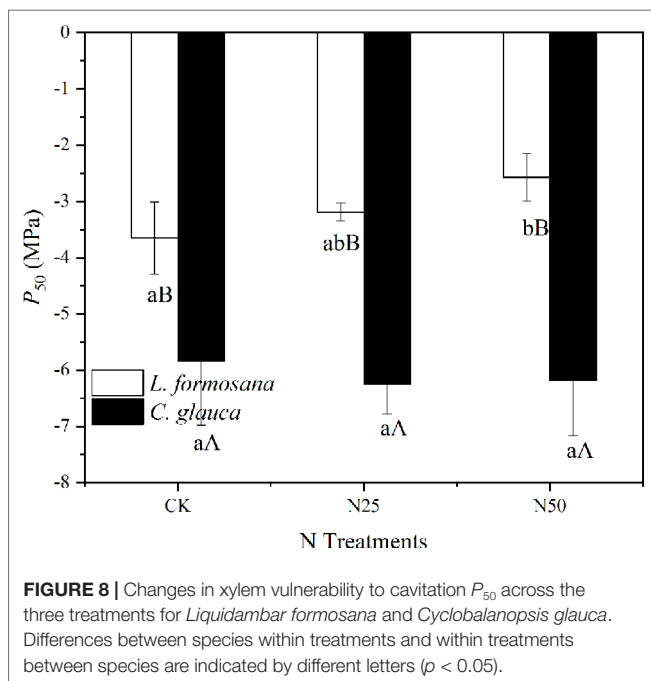
FIGURE 8 | Changes in xylem vulnerability to cavitation P_{50} across the three treatments for *Liquidambar formosana* and *Cyclobalanopsis glauca*. Differences between species within treatments and within treatments between species are indicated by different letters ($p < 0.05$).

formosana leaves of N to chlorophyll synthesis with increasing N fertilization is quite common in deciduous species (Baltzer and Thomas, 2005; Gradowski and Thomas, 2008; Yin et al., 2009). In fact, this evolutionary shift could also be observed in annual herbaceous plants with a similar resource utilization strategy (Feng et al., 2009; Wang et al., 2012a; Mu et al., 2016) but never in evergreen species (Warren and Adams, 2004), which need to invest the N in mechanisms to conserve water and nutrients and to tolerate water and nutrient stress (Warren et al., 2003).

The Effect of N on Photosynthesis

However, even though both species accumulated N in the leaf biomass and *Chl*, the elevated N was not translated to photosynthesis for *C. glauca* (**Table 1**, **Figure 4**). The A_{max} for *L. formosana* was positively promoted by the enhanced N_m and *SLA* ($p < 0.01$, R^2 = 0.27 and 0.17), which is consistent with the resource-limited photosynthesis for most deciduous species in previous studies (Xia and Wan, 2008; Kröber and Bruelheide, 2014; Wooliver et al., 2016). In contrast, the A_{max} for the evergreen *C. glauca* did not respond to N accumulation. The significantly increased *AQY* indicated the enhanced capacity to assimilate CO_2 for both species, which was consistent with the accumulated *Chl* in the N50 treatment across the two species (**Table 1**, **Figure 3**). However, the large proportion of decreased C_i for *C. glauca* (by 42.04%) may imply severe stomatal limitation when the *L. formosana* was compared (11.64%), thus eliminating the N effect on photosynthesis. Indeed, studies have indicated that the effect of nitrogen on photosynthesis of evergreen species will be enhanced by elevated CO_2 (Bauer et al., 2001). Thus, we can expect that the stomatal-limited CO_2 could explain the weak changes of A_{max} for the evergreen *C. glauca*.

Hydraulically Limited Plant Biomass Accumulation

The stomatal limitations did occur for *C. glauca* in the highest N treatments. The g_s in the N50 treatments decreased by 37.5% for *C. glauca* and tended to be less related to the sapwood conductivity (**Figure 5**). In contrast, the g_s tended to be more and more sensitive to the increase of K_S along with the weak decrease (by 8.33%, $p > 0.05$) for *L. formosana*. The K_S for both species increased significantly (by 59.49 and 39.18%). We expected that the reduced g_s may be attributed to the enhanced water lose on the leaf supported by the increased K_S and *SLA*. In dry conditions, the increased *AQY* will raise photosynthesis and leaf transpiration under low light conditions, which further lead to excessive water loss and severe stomatal control for the evergreen *C. glauca* (**Figure 6**). In addition, the increased *SLA* also added to the water loss, which elevated the light acquisition ability as well as the transpiration area. However, stomatal limitation did not occur for *L. formosana*, and a similar increase in *SLA*, *AQY*, and K_S was observed (**Table 1**, **Figure 6**), which was thought to be related to the different water use regulation strategies for the evergreen and deciduous species. Evergreen species tended to rapidly close their stomata in response to excessive water loss to maintain higher leaf water potential in contrast to the deciduous species (**Figure 6**), which is known as isohydric-prone *versus* anisohydric-prone behavior (Kumagai and Porporato, 2012; Klein and Niu, 2014; Siddiq et al., 2017). The first will reduce the risk of damaging xylem cavitation driven by excessive tension in the trees' hydraulic system (Klein and Niu, 2014). However, a consequence of this strategy is that these trees close their stomata in response to even mild water stress—a process that reduces leaf carbon (C) uptake (Siddiq et al., 2017). In our study, the leaf scale photosynthesis was translated into the accumulation of whole tree biomass (by 34.34%) for *L. formosana* in the N50 treatments but not for *C. glauca,* even though the N concentration of plant biomass for both species was apparently elevated. These results indicated that the prevailing seasonal drought did not neutralize the fertilization effect for *L. formosana* but had the inverse effect in *C. glauca*.

It is noted that the increase in biomass observed for *L. formosana* does not imply certain success in species competition. In fact, even though anisohydric trees could allow their leaf Ψ (Ψ_L) to decrease during drought by sustaining relatively high g_s (and thus C assimilation), a greater risk of cavitation in the xylem could ultimately lead to rapid declines in leaf water supply that may affect a range of physiological variables, including photosynthetic capacity and g_s (McDowell et al. 2008; Roman et al., 2015). In fact, the P_{50} of *C. glauca* almost doubled that of *L. formosana*, thus revealing advantages in response to seasonal drought. Furthermore, the elevated N availability tended to enhance the leaf water loss by increasing LAR and weakly changing LMF for both species, while the P_{50} was elevated only for *L. formosana*. Thus, extreme drought events may threaten the survival of *L. formosana via* hydraulic failure (Roman et al., 2015), especially in the context of elevated N availability.

CONCLUSION

In our study, the two species that belong to two different forest types behave distinctly in response to elevated N availability. Both the deciduous *L. formosana* and the evergreen *C. glauca* accumulated N in *Chl*, which led to elevated *AQY* in the leaves. In combination with the increased *SLA* and whole tree leaf area, the transpiration demands were promoted for both species. However, the lower compensation of elevated K_S could not balance the excessive leaf water loss, which lead to decreased g_s for the evergreen *C. glauca*. In contrast, the elevated A_n for the deciduous *L. formosana* accumulated a 34.34% increase in whole tree biomass. However, due to the anisohydric behavior and less negative P_{50}, especially when N was elevated for *L. formosana*, the competitive relationship between the two species is still inconclusive due to the risk of hydraulic failure in the face of the gradually enhanced seasonal drought in the Yangtze River Delta.

DATA AVAILABILITY STATEMENT

All datasets generated for this study are included in the article/supplementary material.

AUTHOR CONTRIBUTIONS

ZZ designed the experiments. YZ, XZ, and ST conducted the experiment, XF, YC, LZ, XL and CW conducted the statistical analyses of data. ZZ and YZ wrote the manuscript. All authors read and approved the final manuscript.

FUNDING

REFERENCES

Álvarez-Yépiz, J. C., Burquez, A., Martinez-Yrizar, A., Teece, M., Yepez, E. A., and Dovciak, M. (2017). Resource partitioning by evergreen and deciduous species in a tropical dry forest. *Oecologia* 183, 607–618. doi: 10.1007/s00442-016-3790-3

Alder, N., Pockman, W., Sperry, J., and Nuismer, S. (1997). Use of centrifugal force in the study of xylem cavitation. *J. Exp. Bot.* 48, 665–674. doi: 10.1093/jxb/48.3.665

Baltzer, J. L., and Thomas, S. C. (2005). Leaf optical responses to light and soil nutrient availability in temperate deciduous trees. *Am. J. Bot.* 92, 214–223. doi: 10.3732/ajb.92.2.214

Barnard, D. M., Meinzer, F. C., Lachenbruch, B., McCulloh, K. A., Johnson, D. M., and Woodruff, D. R. (2011). Climate-related trends in sapwood biophysical properties in two conifers: avoidance of hydraulic dysfunction through coordinated adjustments in xylem efficiency, safety and capacitance. *Plant Cell Environ.* 34 (4), 643–654. doi: 10.1111/j.1365-3040.2010.02269.x

Bauer, G., Berntson, G., and Bazzaz, F. (2001). Regenerating temperate forests under elevated CO2 and nitrogen deposition: comparing biochemical and stomatal limitation of photosynthesis. *New Phytol.* 152, 249–266. doi: 10.1046/j.0028-646x.2001.00255.x

Binkley, D., Ice, G. G., Kaye, J., and Williams, C. A. (2004). nitrogen and phosphorus concentrations in forest streams of the United States. 1. *JAWRA J. Am. Water Resour. Assoc.* 40 (5), 1277–1291. doi: 10.1111/j.1752-1688.2004.tb01586.x

Bobbink, R., Hicks, K., Galloway, J., Spranger, T., Alkemade, R., Ashmore, M., et al. (2010). Global assessment of nitrogen deposition effects on terrestrial plant diversity: a synthesis. *Ecol. Appl.* 20, 30–59. doi: 10.1890/08-1140.01

Brodribb, T., Holbrook, N. M., and Gutierrez, M. (2002). Hydraulic and photosynthetic co-ordination in seasonally dry tropical forest trees. *Plant Cell Environ.* 25, 1435–1444. doi: 10.1046/j.1365-3040.2002.00919.x

Brookshire, E. N. J., Hedin, L. O., Newbold, J. D., Sigman, D. M., and Jackson, J. K. (2012). Sustained losses of bioavailable nitrogen from montane tropical forests. *Nat. Geosci.* 5, 123–126. doi: 10.1038/ngeo1372

Chen, J.-W., Zhang, Q., and Cao, K.-F. (2008). Inter-species variation of photosynthetic and xylem hydraulic traits in the deciduous and evergreen Euphorbiaceae tree species from a seasonally tropical forest in south-western China. *Ecol. Res.* 24, 65–73. doi: 10.1007/s11284-008-0482-4

Choat, B., Ball, M. C., Luly, J. G., and Holtum, J. A. M. (2004). Hydraulic architecture of deciduous and evergreen dry rainforest tree species from north-eastern Australia. *Trees* 19 (3), 305–311. doi: 10.1007/s00468-004-0392-1

Cochard, H., Damour, G., Bodet, C., Tharwat, I., Poirier, M., and Améglio, T. (2005). Evaluation of a new centrifuge technique for rapid generation of xylem vulnerability curves. *Physiol. Plantarum* 124 (4), 410–418. doi: 10.1111/j.1399-3054.2005.00526.x

Curtis, P. S., and Ackerly, D. D. (2008). Introduction to a "Virtual Special Issue" on plant ecological strategy axes in leaf and wood traits. *New Phytol.* 179, 901–903. doi: 10.1111/j.1469-8137.2008.02593.x

Deutsch, C., and Weber, T. (2012). Nutrient ratios as a tracer and driver of ocean biogeochemistry. *Ann. Rev. Mar. Sci.* 4, 113–141. doi: 10.1146/annurev-marine-120709-142821

Devi, A. F., and Garkoti, S. C. (2013). Variation in evergreen and deciduous species leaf phenology in Assam, India. *Trees* 27, 985–997. doi: 10.1007/s00468-013-0850-8

Feng, Y. L., Lei, Y. B., Wang, R. F., Callaway, R. M., Valiente-Banuet, A., Li, Y. P., et al. (2009). Evolutionary tradeoffs for nitrogen allocation to photosynthesis versus cell walls in an invasive plant. *Proc. Nat. Acad. Sci.* 106, 1853–1856. doi: 10.1073/pnas.0808434106

Gradowski, T., and Thomas, S. C. (2008). Responses of Acer saccharum canopy trees and saplings to P, K and lime additions under high N deposition. *Tree Physiol.* 28, 173–185. doi: 10.1093/treephys/28.2.173

Hietz, P., Turner, B. L., Wanek, W., Richter, A., Nock, C. A., and Wright, S. J. (2011). Long-term change in the nitrogen cycle of tropical forests. *Science* 334, 664–666. doi: 10.1126/science.1211979

Hu, Q. P., Guo, Z. H., Li, C. Y., and Ma, L. Y. (2008). Leaf morphology and photosynthetic characteristics of seedlings of a deciduous and an evergreen broad-leaved species under different light regimes in subtropical forests. *Acta Ecologica Sinica* 28, 3262–3270.

Iversen, C. M., and Norby, R. J. (2008). Nitrogen limitation in a sweetgum plantation: implications for carbon allocation and storage. *Can. J. Forest Res.* 38, 1021–1032. doi: 10.1139/x07-213

Kikuzawa, K., Onoda, Y., Wright, I. J., and Reich, P. B. (2013). Mechanisms underlying global temperature-related patterns in leaf longevity. *Global Ecol. Biogeogr.* 22, 982–993. doi: 10.1111/geb.12042

Klein, T., and Niu, S. (2014). The variability of stomatal sensitivity to leaf water potential across tree species indicates a continuum between isohydric and anisohydric behaviours. *Funct. Ecol.* 28, 1313–1320. doi: 10.1111/1365-2435.12289

Kröber, W., and Bruelheide, H. (2014). Transpiration and stomatal control: a cross-species study of leaf traits in 39 evergreen and deciduous broadleaved subtropical tree species. *Trees* 28, 901–914. doi: 10.1007/s00468-014-1004-3

Kröber, W., Heklau, H., and Bruelheide, H. (2015). Leaf morphology of 40 evergreen and deciduous broadleaved subtropical tree species and relationships to functional ecophysiological traits. *Plant Biol.* 17, 373–383. doi: 10.1111/plb.12250

Kumagai, T., and Porporato, A. (2012). Strategies of a Bornean tropical rainforest water use as a function of rainfall regime: isohydric or anisohydric? *Plant Cell Environ.* 35, 61–71. doi: 10.1111/j.1365-3040.2011.02428.x

Liu, X., Zhang, Y., Han, W., Tang, A., Shen, J., Cui, Z., et al. (2013a). Enhanced nitrogen deposition over China. *Nature* 494, 459–462. doi: 10.1038/nature11917

Liu, X., Fan, Y., Long, J., Wei, R., Kjelgren, R., Gong, C., et al. (2013b). Effects of soil water and nitrogen availability on photosynthesis and water use efficiency of *Robinia pseudoacacia* seedlings. *J. Environ. Sci.* 25, 585–595. doi: 10.1016/s1001-0742(12)60081-3

Lu, X., Mao, Q., Gilliam, F. S., Luo, Y., and Mo, J. (2014). Nitrogen deposition contributes to soil acidification in tropical ecosystems. *Glob. Chang. Biol.* 20, 3790–3801. doi: 10.1111/gcb.12665

Lu, X., Vitousek, P. M., Mao, Q., Gilliam, F. S., Luo, Y., Zhou, G., et al. (2018). Plant acclimation to long-term high nitrogen deposition in an N-rich tropical forest. *Proc. Natl. Acad. Sci. U.S.A.* 115, 5187–5192. doi: 10.1073/pnas.1720777115

McDowell, N., Pockman, W. T., Allen, C. D., Breshears, D. D., Cobb, N., Kolb, T., et al. (2008). Mechanisms of plant survival and mortality during drought: why do some plants survive while others succumb to drought? *New Phytol.* 178, 719–739. doi: 10.1111/j.1469-8137.2008.02436.x

Mu, X., Chen, Q., Chen, F., Yuan, L., and Mi, G. (2016). Within-Leaf nitrogen allocation in adaptation to low nitrogen supply in maize during grain-filling stage. *Front. Plant Sci.* 7, 699. doi: 10.3389/fpls.2016.00699

Osazuwa-Peters, O., and Zanne, A. E. (2011). Wood Density Protocol. URL. <http://prometheuswiki.publish.csiro.au/tiki-index.php?page=Wood+density+protocol>. In Prometheus Wiki.

Ouédraogo, D.-Y., Fayolle, A., Gourlet-Fleury, S., Mortier, F., Freycon, V., Fauvet, N., et al. (2016). The determinants of tropical forest deciduousness: disentangling the effects of rainfall and geology in central Africa. *J. Ecol.* 104, 924–935. doi: 10.1111/1365-2745.12589

Palmroth, S., Bach, L. H., Nordin, A., and Palmqvist, K. (2014). Nitrogen-addition effects on leaf traits and photosynthetic carbon gain of boreal forest understory shrubs. *Oecologia* 175, 457–470. doi: 10.1007/s00442-014-2923-9

Pammenter, N.v., and Van der Willigen, C. (1998). A mathematical and statistical analysis of the curves illustrating vulnerability of xylem to cavitation. *Tree Physiol.* 18, 589–593. doi: 10.1093/treephys/18.8-9.589

Pivovaroff, A. L., Santiago, L. S., Vourlitis, G. L., Grantz, D. A., and Allen, M. F. (2016). Plant hydraulic responses to long-term dry season nitrogen deposition alter drought tolerance in a Mediterranean-type ecosystem. *Oecologia* 181, 721–731. doi: 10.1007/s00442-016-3609-2

Pringle, E. G., Adams, R. I., Broadbent, E., Busby, P. E., Donatti, C. I., Kurten, E. L., et al. (2011). Distinct leaf-trait syndromes of evergreen and deciduous trees in a seasonally dry tropical forest. *Biotropica* 43, 299–308. doi: 10.1111/j.1744-7429.2010.00697.x

Roman, D. T., Novick, K. A., Brzostek, E. R., Dragoni, D., Rahman, F., and Phillips, R. P. (2015). The role of isohydric and anisohydric species in determining ecosystem-scale response to severe drought. *Oecologia* 179, 641–654. doi: 10.1007/s00442-015-3380-9

Shipley, B., Lechowicz, M. J., Wright, I., and Reich, P. B. (2006). Fundamental trade-offs generating the worldwide leaf economics spectrum. *Ecology* 87, 535–541. doi: 10.1890/05-1051

Siddiq, Z., Chen, Y.-J., Zhang, Y.-J., Zhang, J.-L., and Cao, K.-F. (2017). More sensitive response of crown conductance to VPD and larger water consumption in tropical evergreen than in deciduous broadleaf timber trees. *Agr. Forest Meteorol.* 247, 399–407. doi: 10.1016/j.agrformet.2017.08.028

Simon, J., Gleadow, R. M., and Woodrow, I. E. (2010). Allocation of nitrogen to chemical defence and plant functional traits is constrained by soil N. *Tree Physiol.* 30, 1111–1117. doi: 10.1093/treephys/tpq049

Sperry, J. S., Christman, M. A., Torres-Ruiz, J. M., Taneda, H., and Smith, D. D. (2012). Vulnerability curves by centrifugation: is there an open vessel artefact, and are 'r' shaped curves necessarily invalid? *Plant Cell Environ.* 35, 601–610. doi: 10.1111/j.1365-3040.2011.02439.x

Takashima, T., Hikosaka, K., and Hirose, T. (2004). Photosynthesis or persistence: nitrogen allocation in leaves of evergreen and deciduous Quercus species. *Plant Cell Environ.* 27, 1047–1054. doi: 10.1111/j.1365-3040.2004.01209.x

Tilman, D., and Isbell, F. (2015). Biodiversity: recovery as nitrogen declines. *Nature* 528, 336–337. doi: 10.1038/nature16320

Wang, M., and Feng, Y. (2005). Effects of soil nitrogen levels on morphology, biomass allocation and photosynthesis in *Ageratina adenophora* and

Chromoleana odorata. China J. Plant Ecol. 29, 697–705. doi: 10.17521/cjpe.20050093

Wang, X.-H., Kent, M., and Fang, X.-F. (2007). Evergreen broad-leaved forest in Eastern China: Its ecology and conservation and the importance of resprouting in forest restoration. *Forest Ecol. Manag.* 245, 76–87. doi: 10.1016/j.foreco.2007.03.043

Wang, D., Maughan, M. W., Sun, J., Feng, X., Miguez, F., Lee, D., et al. (2012a). Impact of nitrogen allocation on growth and photosynthesis of Miscanthus (*Miscanthus × giganteus*). *GCB Bioenergy* 4, 688–697. doi: 10.1111/j.1757-1707.2012.01167.x

Wang, M., Shi, S., Lin, F., Hao, Z., Jiang, P., and Dai, G. (2012b). Effects of soil water and nitrogen on growth and photosynthetic response of Manchurian ash (*Fraxinus mandshurica*) seedlings in northeastern China. *PLoS One* 7, e30754. doi: 10.1371/journal.pone.0030754

Warren, C. R., and Adams, M. A. (2004). Evergreen trees do not maximize instantaneous photosynthesis. *Trends Plant Sci.* 9, 270–274. doi: 10.1016/j.tplants.2004.04.004

Warren, C. R., Dreyer, E., and Adams, M. A. (2003). Photosynthesis-Rubisco relationships in foliage of *Pinus sylvestris* in response to nitrogen supply and the proposed role of Rubisco and amino acids as nitrogen stores. *Trees* 17 (4), 359–366. doi: 10.1007/s00468-003-0246-2

Wooliver, R., Pfennigwerth, A. A., Bailey, J. K., Schweitzer, J. A., and Fox, C. (2016). Plant functional constraints guide macroevolutionary trade-offs in competitive and conservative growth responses to nitrogen. *Funct. Ecol.* 30, 1099–1108. doi: 10.1111/1365-2435.12648

Xia, J., and Wan, S. (2008). Global response patterns of terrestrial plant species to nitrogen addition. *New Phytol.* 179, 428–439. doi: 10.1111/j.1469-8137.2008.02488.x

Xie, Y., Ma, Z., Yang, Q., Fang, X., Zhang, Z., Yan, E., et al. (2012). Coexistence mechanisms of evergreen and deciduous trees based on topographic factors in Tiantong region, Zhejiang Province, eastern China. *Biodivers. Sci.* 20, 159–167.

Xu, W., Luo, X. S., Pan, Y. P., Zhang, L., Tang, A. H., Shen, J. L., et al. (2015). Quantifying atmospheric nitrogen deposition through a nationwide monitoring network across China. *Atmos. Chem. Phys.* 15 (21), 12345–12360. doi: 10.5194/acp-15-12345-2015

Yin, C., Pang, X., and Chen, K. (2009). The effects of water, nutrient availability and their interaction on the growth, morphology and physiology of two poplar species. *Environ. Exp. Bot.* 67, 196–203. doi: 10.1016/j.envexpbot.2009.06.003

Zhang, W., Mo, J., Zhou, G., Gundersen, P., Fang, Y., Lu, X., et al. (2008). Methane uptake responses to nitrogen deposition in three tropical forests in southern China. *J Geophys. Res.-Atmos.* 113 (D11116) 1099–1102. doi: 10.1029/2007jd009195

Zhang, Y. J., Meinzer, F. C., Qi, J. H., Goldstein, G., and Cao, K. F. (2013). Midday stomatal conductance is more related to stem rather than leaf water status in subtropical deciduous and evergreen broadleaf trees. *Plant Cell Environ.* 36 (1), 149–158. doi: 10.1111/j.1365-3040.2012.02563.x

Zhang, Z., Zhou, J., Zhao, X., Zhao, P., Zhu, L., Ouyang, L., et al. (2017). Maximised photosynthetic capacity and decreased hydraulic failure risk during aging in the clump bamboo, *Bambusa chungii. Funct Plant Biol.* 44, 785–794. doi: 10.1071/FP16381

Zhang, X. F. (2006). Atmospheric nitrogen wet deposition and its effects on wetland water environment of Shanghai area. *J. Appl. Ecol.* 17, 1099–1102.

Zhou, G., and Yan, J. (2001). The influences of regional atmospheric precipitation characteristics and its element inputs on the existene and development of dinghushan forest ecosystems. *Acta Ecologica Sinica* 21 (12), 2002–2012.